JOURNAL OF MATERIALS SCIENCE 17 (1982) 347–358

Influence of microstructure on the dynamic fatigue properties of injection-moulded polypropylene

K. WATKINSON
Rubber and Plastics Research Association, Shawbury, Shropshire, UK

A. THOMAS*, M. BEVIS†
Department of Metallurgy and Materials Science, University of Liverpool, Liverpool, UK

A polypropylene copolymer was injection-moulded using several processing conditions and with different gating systems to produce a range of typical spherulitic microstructures. In addition to internal weld lines, some specimens were joined to form external mirror-plate butt-welds. The effect of the different microstructures on the fatigue and impact properties as a function at two test temperatures of 23 and − 10° C are reported. The influence of the different microstructures resulted in significant differences in load-bearing ability.

1. Introduction

The tougher thermoplastics, such as nylon, acetal and polypropylene, are replacing more conventional materials in many load-bearing applications, a good example of which is in the automotive industry. The performance of these materials under long-term loading, however, has not been investigated to any great extent. It has become apparent from the analysis of in-service failures that if the full potential of these thermoplastics in engineering applications is to be realized then the long-term performance of components, and in particular injection-moulded components needs to be more fully understood.

Injection moulding is one of the most important and widely used fabrication processes for moulding a broad range of thermoplastics. It is generally recognized that the final properties of injection-moulded components are strongly dependent on morphology, orientation and stress history [1–4]. Studies of many polymers have demonstrated that mouldings have a skin of molecules that are highly orientated in the flow direction and an essentially unorientated core [5–7]. The molecular orientation in the skin has been observed, in some cases, to cause warpage, skrinkage and premature failure under impact and flexure [8, 9]. The effect of melt temperature and injection pressure on the texture and microstructure of polypropylene has been reported by numerous authors [10–17], but the effect of moulding variables on the long-term mechanical performance has received little attention. In the case of high-density polyethylene, a recent publication [18] reports on the influence of injection-moulded fittings on the fatigue properties of pipeline systems.

The objective of this study was to investigate the influence of moulding variables on the dynamic fatigue performance of polypropylene and to identify factors which cause premature failure. The effect of various types of welds on the performance of the mouldings was also examined.

2. Experimental method

2.1. Material and moulding conditions

The material used for this study was a general-

*Present address: United Kingdom Atomic Energy Authority, Risley, UK.
†Present address: Department of Non-Metallic Materials, Brunel Universtiy, Uxbridge, UK.

0022–2461/82/020347–12$3.20/0

purpose grade of polypropylene copolymer (GWM 101, ICI Plastics Division). The specimens were moulded on a Stubbe SKM 76-110 injection-moulding machine. Three different specimens were produced; a fan-gated plaque, a merging weld plaque and a double-gated fatique bar specimen, as shown in Fig. 1.

The approach adopted during moulding was to vary the melt and mould temperatures in a systematic manner within the range recommended for this grade by the manufacturer and to alter the injection pressures to give satisfactory mouldings. The remainder of the moulding parameters were kept constant. The moulding cycle was monitored and controlled by a Dynisco Peak Cavity Pressure Controller.

The mouldings were coded according to their melt and mould temperatures i.e. a 250/50 specimen was moulded with a melt temperature of 250° C and a mould temperature of 50° C. Specimens were moulded with melt temperatures in the range 190° C to 250° C and mould temperatures from 30° C to 75° C.

2.2. Hot-plate welding

Complete fan-gated or merging weld plaques were hot-plate welded using a mirror-plate pipe welding machine. The edges of the plaques to be welded were milled square and cleaned with acetone and then placed in contact with the hot plate which was maintained at 21° C. Pressure was applied to the plaques for 5 sec until a 1 mm thick bead formed. Subsequently, the pressure was released and the plaques left in contact with the hot plate for a further 90 sec. After the hot plate was removed, the plaques were pressed together and allowed to cool for 5 min.

2.3. Specimen preparation for dynamic fatigue and microscopy

Specimens for dynamic fatigue testing were milled from the injection-moulded plaques at various angles to the injection direction. No coolant was used during machining. Specimens for light microscopy were prepared by sledge microtomy.

2.4. Dynamic fatigue machines

The majority of the results were obtained from experiments on a four-point bending machine which deformed the specimens under conditions of constant applied load. Some experiments were conducted using cantilever beam bending machines. Two versions of this machine were designed, one to fatigue the specimens by constant applied strain from an eccentric cam. A few experiments were conducted using uniaxial tension compression. The four-point bending experiments used plain rectangular specimens and the cantilever and unaxial experiments used waisted specimens.

All the fatigue experiments were conducted at a frequency of 2 Hz to avoid failures caused by self heating.

3. Results

3.1. The as-moulded microstructures

Thin (210 μm) through thickness sections were microtomed from the centre of fan-gated plaques and were examined by polarized light microscopy.

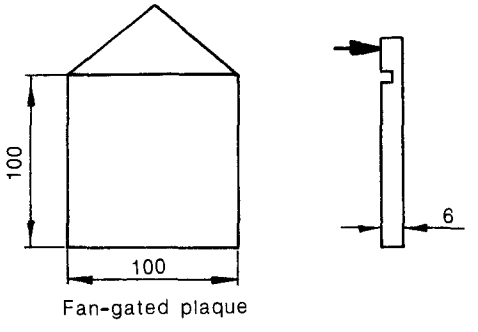

(a) Fan-gated plaque

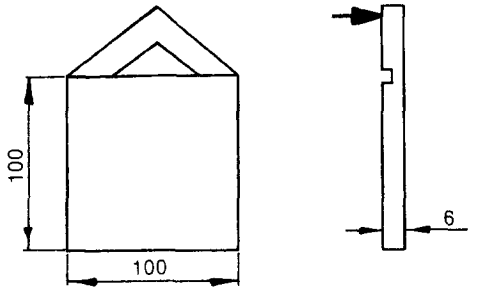

(b) Merging-weld plaque

Figure 1 Geometry of plaque and fatigue bar mouldings: (The injection points are indicated by bold arrows). Dimensions in millimetres. (a) Fan-gated plaque; (b) merging-weld plaque; (c) double-gated fatigue bar.

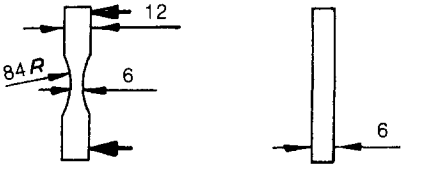

(c) Double-gated fatigue bar

Representative micrographs moulded at two moulding temperatures are shown in Figs 2 and 3. The light micrographs showed that over this range of moulding temperatures, the plaques exhibited the skin–core morphology that is characteristic of many grades of polypropylene. The plaques moulded at 190° C showed the formation of many Type III, negatively bi-refringent spherulites, which are characteristic of the metastable hexagonal crystal form [19, 20]. These spherulites form throughout the bulk of the plaque cross-section along the lines of shear.

The microstructures of the plaques, at all moulding temperatures, can be described in terms of a skin–shear-zone–core model as previously described by Kantz *et al.* [10]. The skin consisted of molecules that were highly orientated in the injection direction, as shown by a uniform extinction of the first-order white polarization colour when the specimen was rotated in the plane of the microscope stage. There was little or no evidence of any crystalline development in the skin for any of the moulding temperatures. The shear zones in the plaque consisted of a large number of Type III spherulites many of which had the appearance of row nucleation, and increased in size towards the centre of the moulding. The core, which made up the bulk of the volume in the injection mouldings, contained larger but randomly sized spherulites. With the exception of the row-nucleated Type III

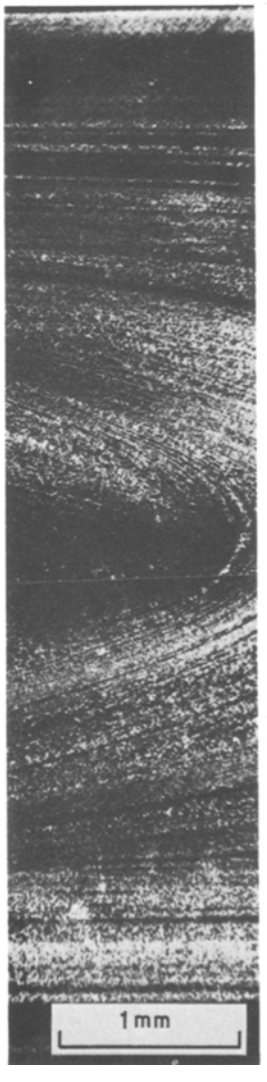

Figure 2 (left) A section through the thickness of a 190/50 plaque.

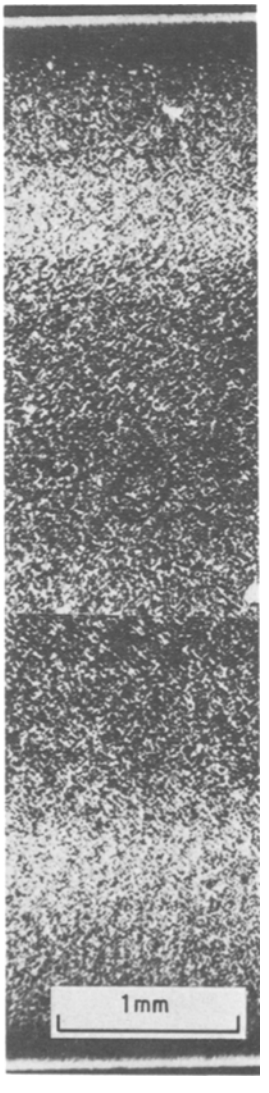

Figure 3 (right) A section through the thickness of a 250/50 plaque.

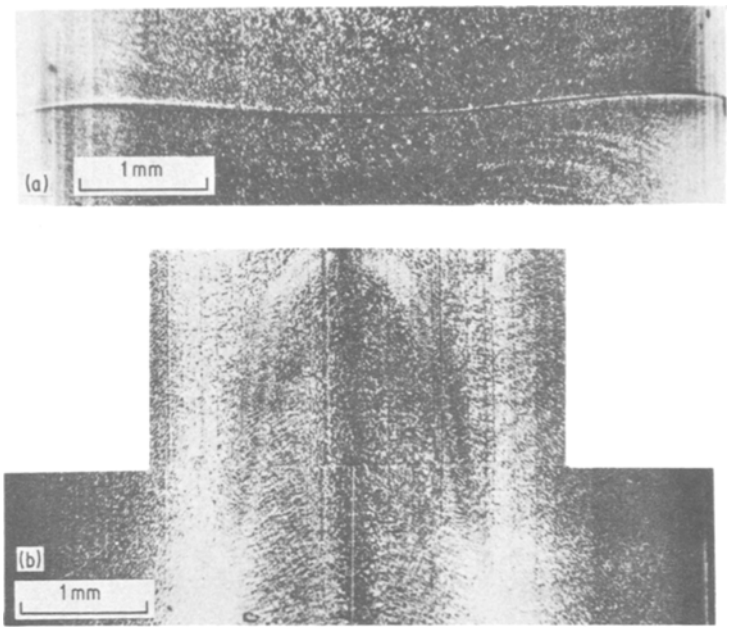

Figure 4 Microstructure of double-gated flexural fatigue bars moulded at (a) 190/50, (b) 230/50.

spherulites in the 220° C mouldings, the spherulites in this zone were the positively-bi-refringent Type I variety which is characteristic of the stable, monoclinic polymorph.

The volume fractions of both the skin and shear zones increase markedly with decreasing melt temperature. The same effect has been reported by Kantz *et al.* [10] for homo- and copolymerized polypropylene. Fig. 4 shows a typical through-thickness section obtained from the centre of a fatigue bar specimen. Over the whole range of moulding temperatures the fatigue bars showed the characteristic "skin–core" morphology, but the weld microstructure varied with moulding temperature. The weld line in specimens moulded at 190° C are characterised by the formation of columnar growth along the weld lines, a feature is shown more clearly in Fig. 5. At the higher moulding temperatures (210° C and 230° C) the weld line could only be identified by a change in the size and appearance of the spherulites within the specimen, giving a so-called "heat-affected zone". For all the specimens the weld line appeared as a small notch within the skin at the specimen surface.

Figs 6 and 7 show micrographs of the structure of through-thickness sections of merging weld plaques. The weld lines in plaques moulded at 190° C were characterized by columnar-type spherulite growth. This can be associated with the merging of the flow fronts at too low a temperature to allow substantial fusion of polymer across the boundary. The "weld line" than acts as a planar nucleation site giving rise to columnar growth.

Plaques moulded at 220° C and 250° C did not show the columnar growth pattern at the weld line, but the position of the weld line along the length of the flow path could be identified by a change in microstructure.

Through-thickness sections of the area around the weld line of hot-plate welded plaques were examined by transmitted light microscopy. Fig. 8 shows a section of the weld formed between two 220/50 plaques. The shear zones are clearly evident along most of the weld face. Only in the centre of the plaques is there a continuous semicrystalline spherulite structure as a result of the lower rate of cooling and lower shear during fabrication. The

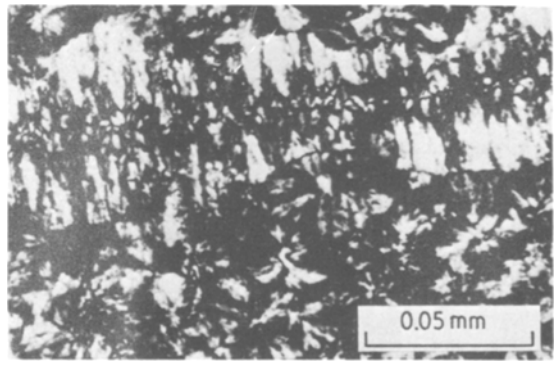

Figure 5 The microstructure at the centre of the weld line in a 190/50 double-gated flexural fatigue bar.

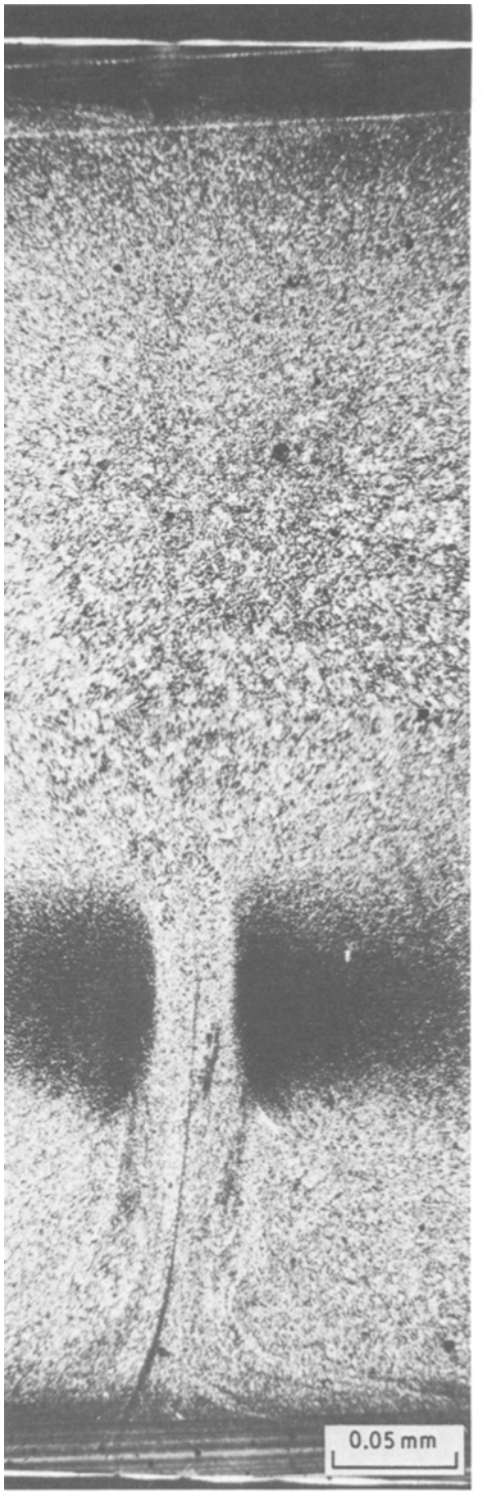

Figure 6 A section through the thickness of a 190/50 merging-weld plaque viewed towards the gate.

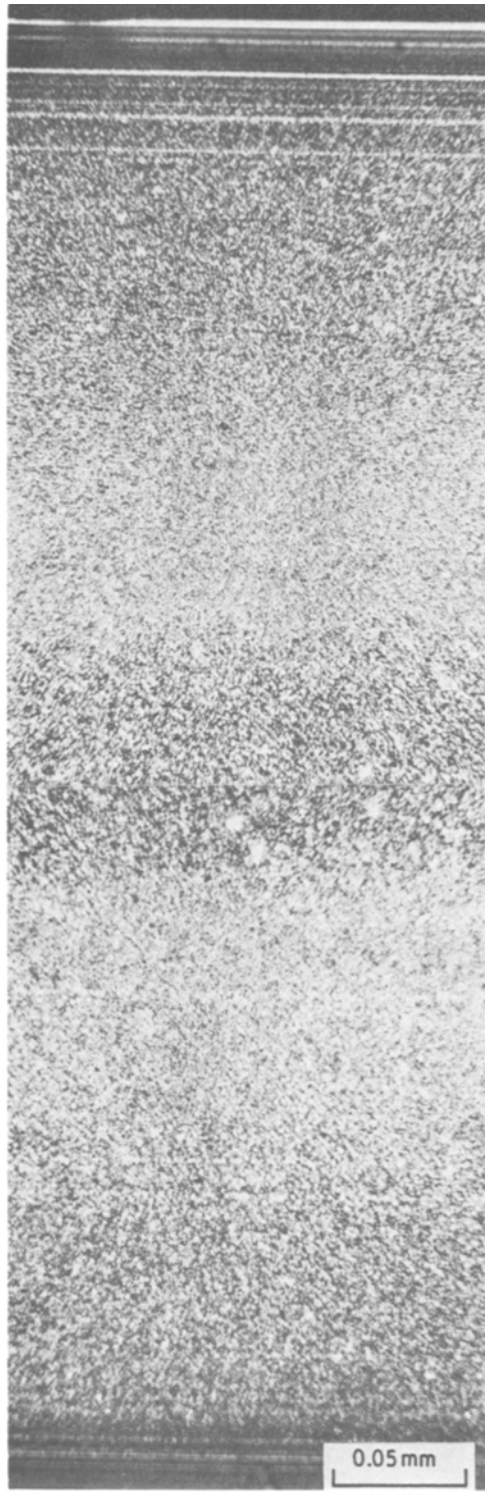

Figure 7 A section through the thickness of a 250/50 merging-weld plaque viewed towards the gate.

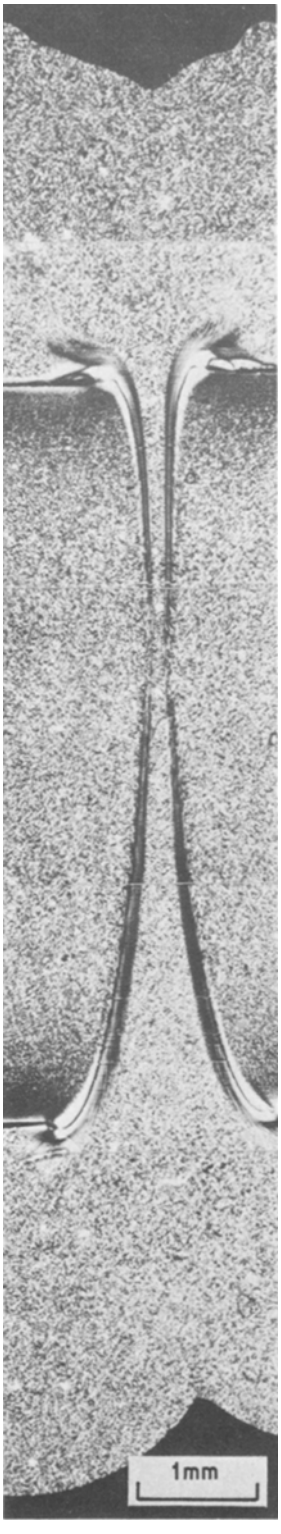

Figure 8 A through-thickness section through the weld formed by hot-plate welding two 220/50 plaques. The resultant beads can be clearly seen at the top and bottom.

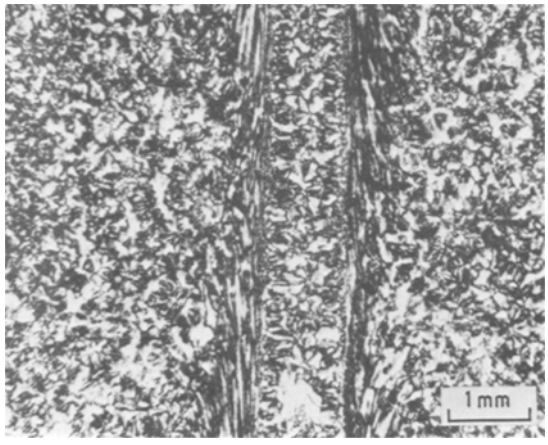

Figure 9 An enlargement of the centre of the weld shown in Fig. 8.

beads have folded back over the plaque surface, but have not formed a molecular bond with the plaque. Fig. 9 shows the weld structure at the centre of the plaques. A similar section through a weld formed between a 220/50 merging weld plaque and a 250/50 plaque showed that the microstructures on the two sides of the weld line were different due to the internal merging weld.

3.2. Dynamic fatigue studies

Experiments were performed on specimens cut at various angles from plaques moulded at three dif-

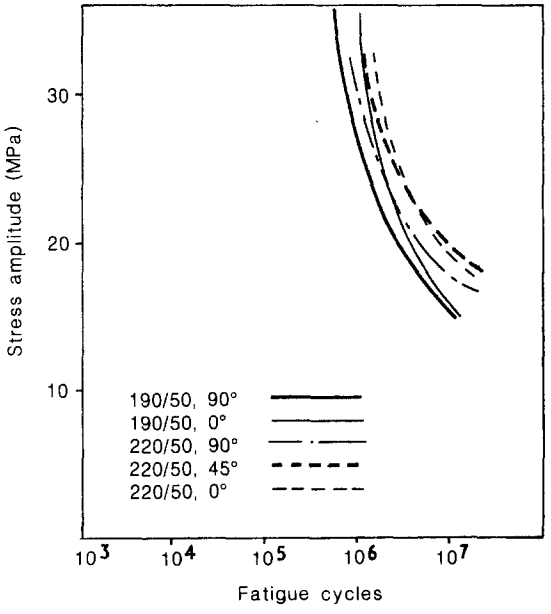

Figure 10 σ–N diagram. Fatigue: four-point bending, constant stress; waveform: sinusoidal, 2Hz.

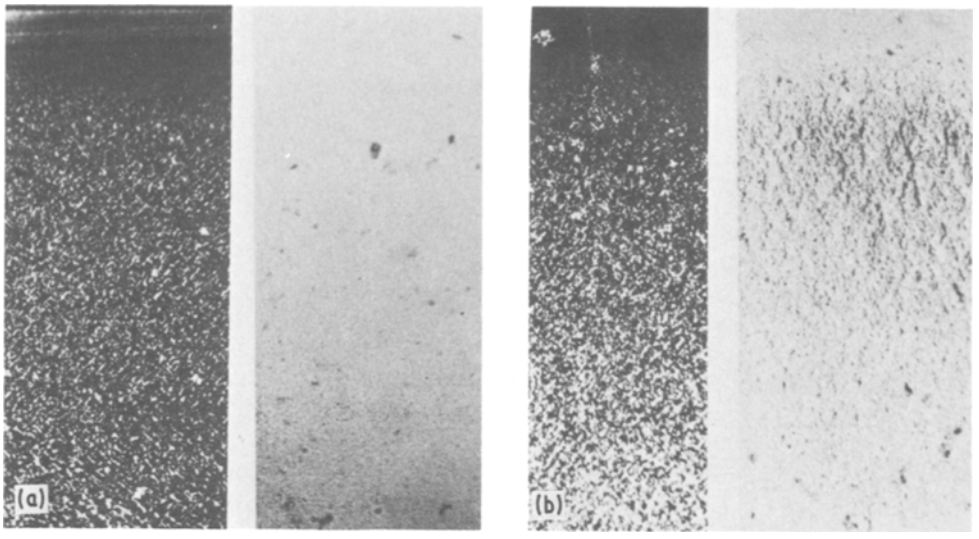

Figure 11 Micrographs in polarized and unpolarized light of fatigue damage in plaques. (a) 250/50 plaque, 100 cycles; (b) 190/50 plaque, 1000 cycles; (c) 250/50 plaque, 1000 cycles.

ferent temperatures to establish the effect of orientation and moulding history on fatigue performance. Fig. 10 shows the results of fatigue in four-point bending in the stress control mode. A small but discernable difference is seen in performance between 190/50 specimens cut at 0° and 90° to the injection direction. This difference amounts to about 3 % in load-bearing ability after 10^7 cycles. A larger difference in fatigue performance with orientation can be seen in the 220/50 mouldings. The performance of the specimens cut at 45° to the injection direction is curious as intuitively it would be expected that the specimen oriented at 0° would be the most fatigue resistant. Comparing the fatigue behaviour of 190/50 specimens and 220/50 specimens it can be seen that a 30° C increase in melt temperature can yield a 25 % increase in load-bearing performance.

This improvement in fatigue performance can be attributed to the more uniform microstructure of the 220/50 plaques. Examination of the microstructure of fatigue specimens showed that damage occurs initially in regions of high shear. Fig. 11 shows micrographs in polarized and unpolarized light of specimens that have been fatigued to various lifetimes. The onset of damage occurs initially in the sub-skin zones (shear zone) and it occurs earlier in the 190/50 specimens. No damage appears to be created in the skin for quite an appreciable period, and when damage does occur in the skin it is caused by shear banding.

A similar response to fatigue loading under conditions of constant strain is observed for 190/50 and 250/50 plaques cut at 90° to the injection direction (Fig. 12). At 10^7 cycles the difference in strain acceptance between the 190/50 and the 250/50 is 0.025 to 0.030. From these results the effect of moulding conditions on dynamic fatigue performance does not seem to be particularly significant within the range of moulding conditions examined, and particularly at low loads which relate more closely to in-service loading histories.

This may be explained by the relative skin thick-

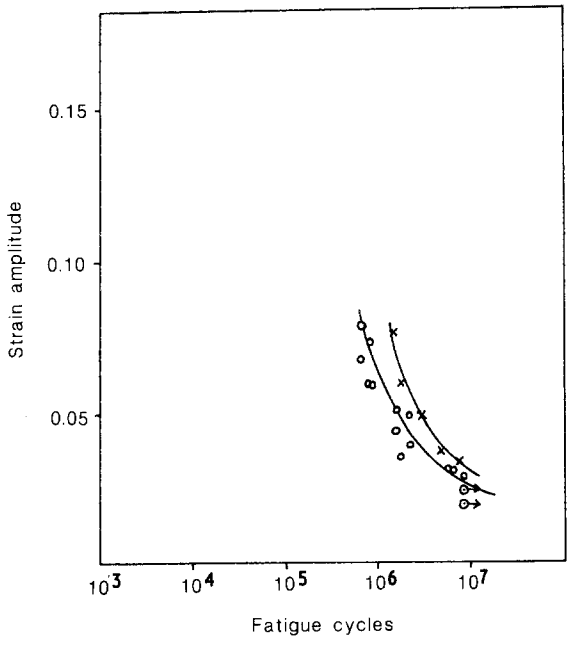

Figure 12 ϵ–N diagram. Fatigue: cantilever, constant strain; waveform: sinusoidal, 2Hz; specimens: plaques 90°; o, 190/50; ×, 250/50.

ness and the fatigue mode used. Microscopical examination of fatigue damaged specimens has shown that the damage initiates in the skin–core boundary layer. The skin thickness is about 0.19 mm for the 190/50 mouldings and about 0.07 mm for the 250/50 mouldings. Consequently, in flexural or bending fatigue for a given normal stress the skin–core boundary of a 220/50 specimen, experiences a higher stress than a 190/50 specimen.

To a good approximation the microstructure and hence (it is reasonable to assume) the properties of the core material are independent of moulding temperature in the range 210° C to 250° C. Consequently, the core material of each of the different mouldings will have a similar crack propagation rate. This implies that the observed differences in fatigue life are primarily due to differences in crack initiation which are known to be influenced by microstructure and hence moulding conditions.

A common feature in many injection-moulded components is a weld or knit line formed when two flow fronts meet. These flow fronts may have originated from different gates or as a result of the primary flow front splitting to encompass an obstruction such as a pin. It has long been known that a weld line introduces a plane of weakness in a moulding but apart from a few studies on short-term effects such as impact strength no real assessment has been made of the reduction in long term performance caused by the presence of a weld line.

The fatigue performance of butt welds created when two flow fronts flowing in opposing directions meet, was assessed as a function of temperature and moulding conditions (Fig. 13). At the highest strains used, which approached the yield strain, there is quite a clear trend in the fatigue performance of the specimens with respect to their moulding conditions. At these strain levels the applied fatigue loading exploits the most severe inherent defects within the weld and even a reduction in test temperature of 30° C does not significantly alter the fatigue performance. At lower strains however, the trend in improved fatigue performance with increase in melt temperature becomes less obvious. This implies that the defects which are responsible for ultimate failure are not exclusively associated with the major inherent moulded-in defect, i.e. the weld line, but are created or developed during fatigue loading. The weld line could act as a notch or stress concentrator which effectively reduces the initiation period of crack formation.

Fig. 14 compares the fatigue performance of double-gated fatigue bars and specimens cut from plaques. The deleterious influence of the weld on fatigue performance is more clearly shown than is

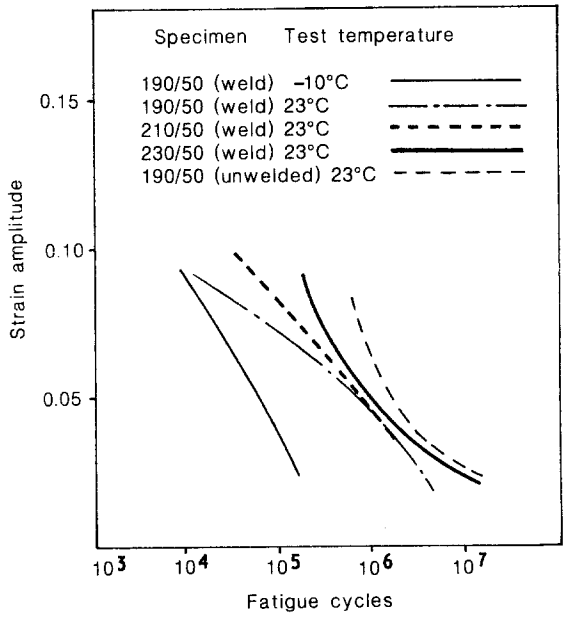

Figure 13 ϵ–N diagram. Fatigue: cantilever, constant strain; waveform: sinusoidal, 2 Hz; specimens: double-gated fatigue bars.

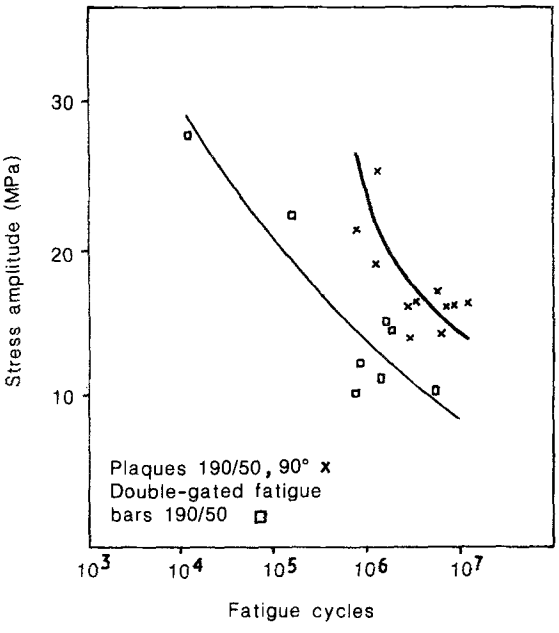

Figure 14 ϵ–N diagram. Fatigue: cantilever, constant stress; waveform: square, 2HZ; specimens: double-gated fatigie bars 190/50.

the case of fatigue in the constant-strain mode. Nevertheless, there remains a trend towards increasingly similar performance at long times.

Fig. 15 shows micrographs of the area around the weld line of double-gated fatigue bar specimens that had been given histories of between 10^2 and 10^5 cycles. The micrographs show that the damage induced by fatigue loading is localized to the area immediately surrounding the weld line. As in the case of the fan-gated plaques the damage occurs initially in the sub-skin region and even after 10^5 cycles, there is little evidence of damage within the skin.

Another type of weld which was examined was a merging weld formed when two flow fronts that are moving in the same direction coalesce. Fig. 16 shows the effect of moulding conditions and specimen orientation on fatigue performance. As expected, the effect of orientation is more evident than in the case of fan-gated plaques. The results indicate that there is an 18% difference in load-bearing ability between specimens orientated at 0° or 90° to the weld line for 250/50 specimens and 14% for 220/50 specimens. Surprisingly, the fatigue of the 220/50 specimens was superior to that of the 250/50 specimens. On the basis of the results obtained on double-gated fatigue bars, it was expected that an increase in melt temperature would lead to an increase in fatigue resistance. Microstructural analysis showed that there was a higher proportion of shear-nucleated Type III spherulites along the weld line of the 220/50 specimens. It appears therefore that a reasonable degree

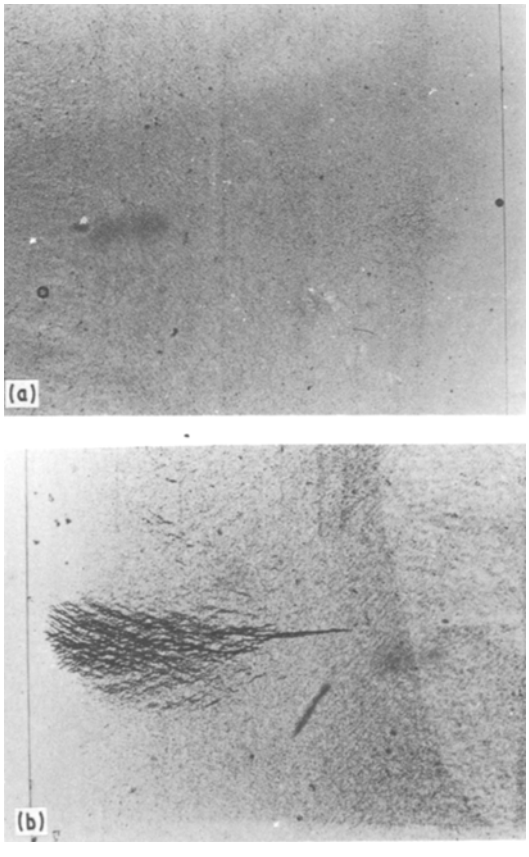

Figure 15 Fatigue damage at the weld line of 210/50 double-gated fatigue bars subjected to fatigue of (a) 100 cycles, (b) 1000 cycles. (c) 100,000 cycles.

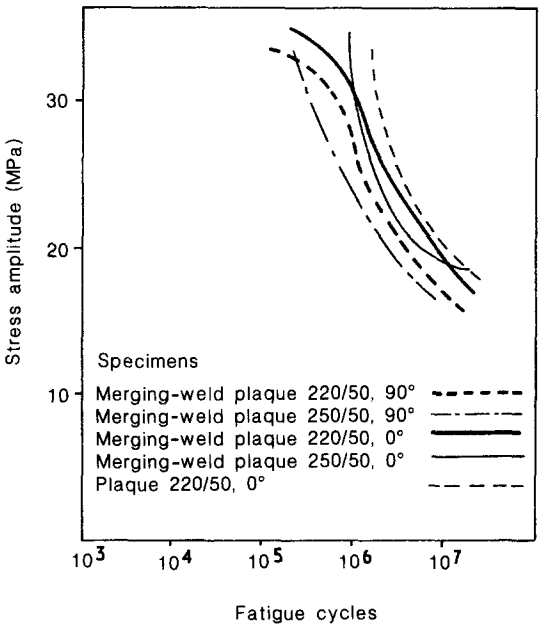

Figure 16 ϵ–N diagram. Fatigue: four-point bending, constant stress; waveform: sinusoidal, 2 Hz; specimens: merging-weld plaques.

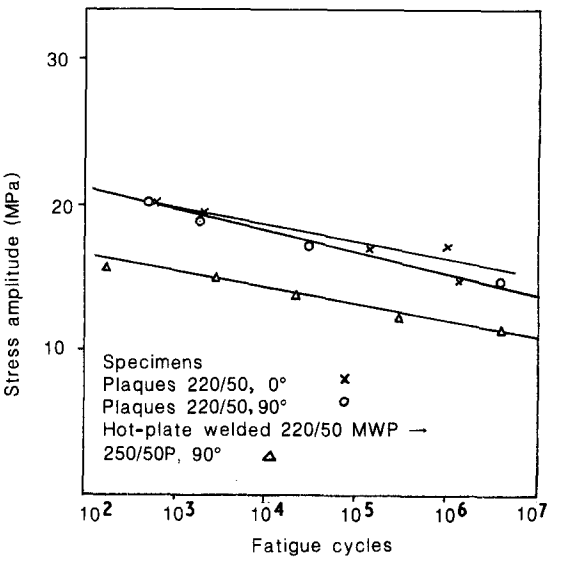

Figure 17 ϵ–N diagram. Fatigue: uniaxial tension (compression) constant stress; waveform: square, 2 Hz.

of shear between the flow fronts is necessary in order to obtain a reasonable weld.

In the long term, the influence of the weld on fatigue performance becomes less apparant, as was observed in the case of the double-gated bars. When measured at 90° the presence of the weld reduces the load-bearing ability by about 5 % compared to a plain specimen.

Hot-plate welds made between plaques were tested at 90° to the weld direction in uniaxial tension compression. Fig. 17 shows the comparative performance of 220/50 plaques cut at 0° and 90° to the injection direction, and hot-plate welded plaques (220/50 merging weld to 220/50 plaques). The load-bearing ability of the hot-plate welded plaques is only about 78 % of that of an unwelded specimen.

3.3. Impact strength and tensile yield stress as a function of fatigue

In order to investigate the effects of fatigue on other mechanical properties a number of experiments were conducted on double-gated fatigue bars which had been given fatigue histories. Fig. 18 shows the effect of fatigue life on the weld-line impact strength as a function of moulding conditions. Data generated by the manufacturers show that the impact strength of GWM 101 at 23° C with a 2 mm radius notch is about 14.7 kJ m^{-2}. A butt-weld line in a moulding produced at 210/50 would appear therefore to act as a 2 mm radius notch. Fig. 18 shows that the impact strength of the mouldings remain almost constant for lifetime up to 5 x 10^5 cycles, before decreasing. This behaviour implies that the defects or damage created by fatigue loading at this strain level are insensitive to impact loading and are less severe than the initial (moulded-in) defects. After fatigue cycling beyond 5 x 10^5 cycles, either new defects are created or the initial moulded-in defects have been developed to a point where they influence the impact strength. It is significant that the impact strength of all the

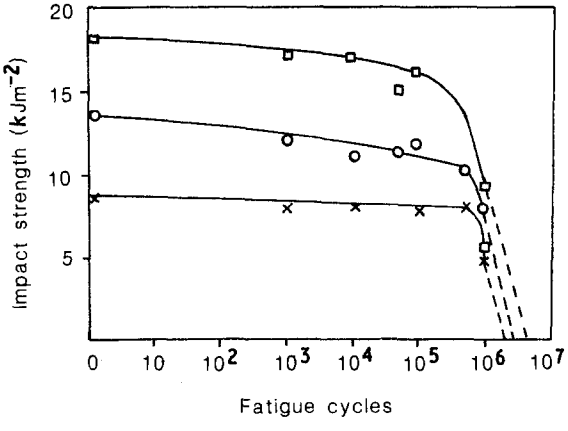

Figure 18 Charpy impact strength as a function of fatigue history and moulding conditions. Fatigue: cantilever, constant strain ± 0.03; waveform: sinusoidal, 2Hz; specimens: double-gated fatigue bars: ×, 190/50; ○, 210/50; □, 230/50.

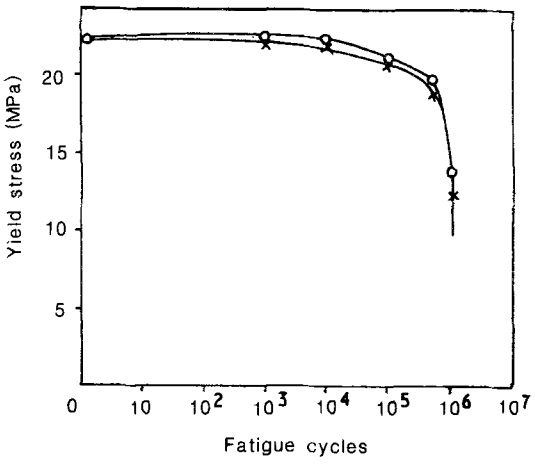

Figure 19 Tensile yield stress as a function of moulding conditions and fatigue history. Fatigue: cantilever, constant strain ± 0.061; waveform: sinusoidal ± 0.061; specimens: double-gated fatigue bars; x, 190/50; o, 230/50.

specimens begins to decrease at about the same fatigue life, irrespective of moulding conditions, indicating that the critical defect size (the size of defect which affects impact strength) is a function of time under load and that therefore its growth is controlled by time-dependent viscoelastic properties. While this evidence is insufficient for absolute proof, it would support the view that the defects that are responsible for ultimate failure are created during load cycling rather than existing moulded-in defects becoming more severe.

A similar experiment was performed using tensile yield stress as the monitor of performance after fatigue cycling (Fig. 19) and a similar response to fatigue was noted. There was no detectable change in the yield stress for lifetime up to 5×10^5 cycles. thereafter, a rapid fall in yield stress occurred. The commencement of the faill in yield stress occurred after the same fatigue history as in the case of the fatigue-impact experiments. Varying the injection moulding conditions does not appear to have any appreciable effect on the tensile strength of the specimens.

4. Conclusions

Optical analysis of through thickness and in-plane sections of plaque and double-gated fatigue bar has shown that a precise and reproducible microstructure exists which is process dependent. Microstructural examination of specimens that had been given various fatigue histories showed that the onset of fatigue damage could be associated with certain structural features present in the moulding. A microstructural technique of this type therefore, could be useful in screening applications during prototype mouldings in order to optimize the performance of new components.

Dynamic fatigue performance was used as the principal monitor of the effect of a number of process and design variables on performance. It was found that within the range of moulding conditions and specimens examined the effect of orientation induced by moulding on fatigue performance was small, leading to about a 3% difference in load-bearing ability when comparing specimens cut parallel with and at right angles to the flow direction. Increasing the melt temperature from 190° C to 290° C improved the load-bearing ability by up to 25%. The influence of weld or knit lines on fatigue varied according to their type. An internal butt weld had the most severe effect, reducing the load-bearing ability by 40%. Merging welds caused only a 5% reduction and hot-plate welds a 22% reduction in load-bearing ability.

Monitoring the development of fatigue damage by impact or yield stress studies revealed an appreciable apparent latent period of damage initiation followed by a rapid decrease in performance. This work is currently being extended to examine the effect of pigments on long-term mechanical performance. It is known that some pigments have a significant effect on the short-term impact and tensile performance, mainly through modification of the crystal matrix. In addition, aspects of aging and weathering on long-term performance will be investigated.

Acknowledgments

The authors are indebted to the Science Research Council for the award of a Research Grant in support of the reported work and to ICI plastics Division for the supply of polypropylene copolymer. The injection moulding and microstructure characterization was carried out at Liverpool University and the mechanical testing at the Rubber and Plastics Association.

References

1. C. E. BAYER and R. S. SPENCER, "Rheology 3" edited by F. R. Kirich (Academic Press, New York and London, 1969) p. 413.
2. R. S. STEIN, *SPE Trans.* 4 (1964) 178.
3. V. TAN and M. R. KAMAL. *SPE* **34** ATC (1976) 339.
4. Z. BAKERDJIAN and M. R. KAMAL, *Polymer Eng. Sci.* **17** (1977) 96.

5. R. M. OGORKIEWICZ, "Thermoplastics: Effect of Process" (Iliffe, London, 1969).
6. E. S. CLARK, *SPE* Division Technical Conference, Downington (1973) p. 98.
7. J. BOWMAN, N. HARRIS and M. BEVIS *J. Mater. Sci.* **10** (1975) 63.
8. A. C. MORRIS, *Plastics and Polymer* **36** (1968) 433.
9. B. MAXWELL. *J. Polymer Sci.* **C9** (1965) 43.
10. M. R. KANTZ, H. O. NEWMAN and F. H. STIGALE. *J. Appl. Polymer. Sci.* **16** (1972) 1249.
11. M. R. KANTZ. SPE Division Technical Conference, Downingtown, (1973) p. 86.
12. M. FUJIYAMA and H. AWAYA, *J. Appl. Pol. Sci.* **21** (1977) 3291.
13. D. R. FITCHMUN and Z. MENCIK, *J. Pol. Sci. A-2* **11** (1973) 951.
14. Z. MENCIK and D. R. FITCHMUN, *ibid.* **11** (1973) 973.
15. D. E. SCHERPEREEL, *Plast. Eng.* **29** (1973) 46.
16. S. J. HERKE, C. E. SMITH and R. F. ABOTT, *Polymer. Eng. Sci.* **15** (1975) 79.
17. E. S. CLARK, *ACS Pol. Prep.* **14** (1973) 268.
18. M. B. BARKER, J. BOWMAN and M. BEVIS, *J. Mater. Sci.* **15** (1980) 265.
19. H. D. KEITH, F. J. PADDEN, N. M. WALKER and M. W. WYCKOFF, *J. Appl. Phys.* **30** (1959) 1485.
20. P. GEIL, "Polymer Single Crystals", (Interscience, New York, 1963).

Received 5 June
and accepted 18 June 1981